

Structural, optical and magnetic properties of $(\text{In}_{0.90}\text{Sn}_{0.05}\text{Cu}_{0.05})_2\text{O}_3$ nanoparticles

S. Harinath Babu, S. Kaleemulla', N. Sai Krishna, N. Madhusudhana Rao, M. Kuppan, C. Krishnamoorthi, Girish M. Joshi, R. K. Kotnala, and J. Shah

Citation: **1731**, 130005 (2016); doi: 10.1063/1.4948111

View online: <http://dx.doi.org/10.1063/1.4948111>

View Table of Contents: <http://aip.scitation.org/toc/apc/1731/1>

Published by the [American Institute of Physics](#)

Structural, Optical and Magnetic Properties of $(\text{In}_{0.90}\text{Sn}_{0.05}\text{Cu}_{0.05})_2\text{O}_3$ Nanoparticles

S. Harinath Babu^a, S. Kaleemulla^{a*}, N. Sai Krishna^a, N. Madhusudhana Rao^a,
M. Kuppan^a, C. Krishnamoorthi^a, Girish M. Joshi^a, R.K. Kotnala^b, J. Shah^b

^a*Thin Films Laboratory, School of Advanced Sciences, VIT University, Vellore – 632 014, Tamilnadu, India*

^b*CSIR-National Physical Laboratory, Dr. K. S. Krishnan Road, New Delhi, India*

**Email: skaleemulla@gmail.com*

Abstract. This study examined structural, optical and magnetic properties of ITO ($\text{In}_{0.95}\text{Sn}_{0.05}$)₂O₃ and Cu doped ITO ($\text{In}_{0.90}\text{Sn}_{0.05}\text{Cu}_{0.05}$)₂O₃ nanoparticles synthesized by solid state reaction method. The synthesized nanoparticles were subjected to structural, optical and magnetic studies. The structural properties of the nanoparticles were carried out using XRD, Raman, FT-IR characterization techniques. Optical properties of the samples were studied using UV-Vis-NIR spectrophotometer. The magnetic measurements were carried out using vibrating sample magnetometer. The ITO ($\text{In}_{0.95}\text{Sn}_{0.05}$)₂O₃ nanoparticles exhibited room temperature ferromagnetism with clear hysteresis loop. The strength of magnetization decreased in Cu doped ITO ($\text{In}_{0.90}\text{Sn}_{0.05}\text{Cu}_{0.05}$)₂O₃. The ITO nanoparticles were also exhibited ferromagnetism at 100 K with a magnetic moment of 0.02 emu/g.

Keywords: Nanoparticles, Cu doped ITO, solid state reaction, Ferromagnetism

PACS: 73.50.Td, 75.50.Pp, 75.47.Lx, 75.50.Dd

INTRODUCTION

Since the discovery of ferromagnetism in Mn doped ZnO [1] with Curie temperature above room temperature, much focus is being put on wide band gap oxide semiconductors. Intensive research work had been carried out on transitional metal doped oxide semiconductors such as ZnO, TiO₂ and SnO₂ [2]. But results were quite controversial. In few research articles it was reported that the observed ferromagnetism was due to metal clusters/secondary phases whereas in other research papers it was reported that the observed ferromagnetism was intrinsic in nature and explained by considering different model such carrier mediated interactions [3], double exchange interactions [4] bound polaron magnetic (BPM) model [5]. Reports on the Cu doped ITO nanoparticles are meagre. Hence an attempt is made here for the synthesis and characterization of ITO and Cu doped ITO nanoparticles.

EXPERIMENTAL

ITO ($\text{In}_{0.95}\text{Sn}_{0.05}$)₂O₃ and Cu doped ITO ($\text{In}_{0.90}\text{Sn}_{0.05}\text{Cu}_{0.05}$)₂O₃ nanoparticles were prepared

by simple standard solid state reaction method. In a typical synthesis, commercially available In₂O₃, SnO₂ and Cu₂O (Sigma-Aldrich, 99.999% pure) powders were taken in desired ratios and mixed in Agate mortar and ground thoroughly for 16 hours using pestle. The ground fine stoichiometric samples were loaded into a small one end closed quartz tube of diameter 10 mm and length 10 cm, which was then enclosed by a bigger quartz tube of diameter of 2.5 cm and length of 75 cm with a provision to allow unwanted vapours to escape from the reaction chamber and it was evacuated to a pressure of 2×10^{-3} mbar using a rotary vane pump. The complete set up was placed in horizontal tubular microprocessor controlled furnace and heated for several hours at different temperatures. After that the samples were subjected to their structural and optical properties.

RESULTS AND DISCUSSION

Structural Properties

Fig.1 shows the X-ray diffraction patterns of the Cu₂O, In₂O₃, Sn doped In₂O₃ (ITO) and Cu doped In₂O₃ nanoparticles, respectively. The X-ray diffraction patterns of Cu₂O, SnO₂ are provided here

to confirm that no secondary phases related to impurities in any form are present.

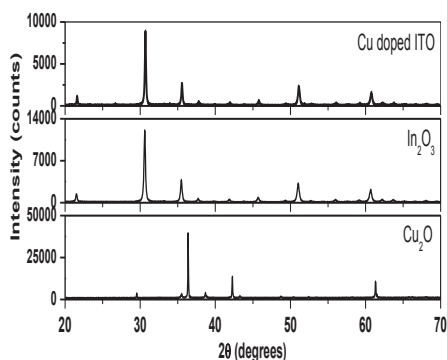


FIGURE 1. X-ray diffraction patterns of Cu_2O , In_2O_3 , Cu doped ITO nanoparticles.

All the diffraction peaks were exactly coincided with cubic structure of In_2O_3 . The XRD patterns conformed that the impurity phases were not observed in In_2O_3 nanoparticles. The diffraction peaks such as (2 1 1), (2 2 2), (4 0 0), (4 1 1), (3 3 2), (4 3 1), (5 2 1), (4 4 0), (4 3 3), (6 1 1), (5 4 1), (6 2 2), (6 3 1), (4 4 4), (5 4 3), (6 4 0), (7 2 1), and (6 4 2) were found in all the In_2O_3 nanoparticles among which (2 2 2) peak was predominant. All the indexed peaks exactly coincided with the cubic structure of In_2O_3 (JCPDS No. #06-0416). Similar diffraction peaks were also observed for ITO and Cu doped ITO nanoparticles. The crystallite size was calculated using Scherer's relation and found that it was about 30 nm.

Optical Properties

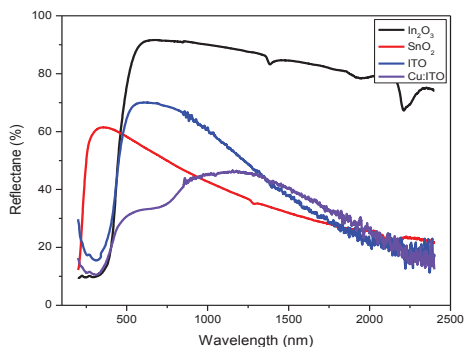


FIGURE 2. Diffuse reflectance spectra of In_2O_3 , SnO_2 , ITO and Cu doped ITO nanoparticles.

The absorption coefficient was calculated using Kubelka-munk function relation [6]. Fig. 3 shows

the optical band gap of the $(\text{In}_{0.95-x}\text{Sn}_{0.05}\text{Ni}_x)_2\text{O}_3$ nanoparticles. The optical band gap (E_g) was obtained by plotting $(\alpha h\nu)^2$ versus the photon energy ($h\nu$) and by extrapolating the linear region ($\alpha = 0$). The optical band gap was estimated using the Tauc relation [7]. The band gap of 3.12 eV was found for the $(\text{In}_{0.90}\text{Sn}_{0.05}\text{Cu}_{0.05})_2\text{O}_3$ nanoparticles

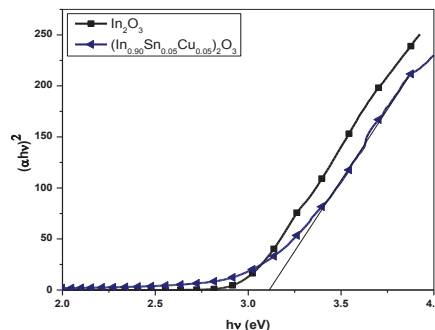


FIGURE 3. Plots of $(\alpha h\nu)^2$ versus $h\nu$ of the In_2O_3 and Cu doped ITO nanoparticles.

Magnetic properties

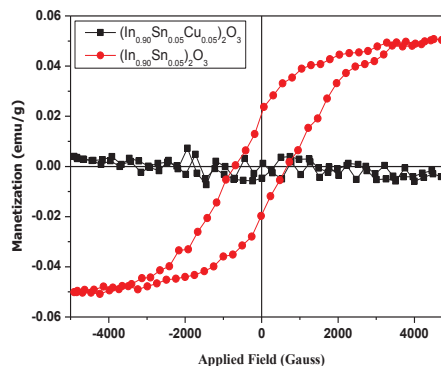


FIGURE 4. Magnetic hysteresis loops (M-H) of ITO and Cu doped ITO nanoparticles at room temperature.

Fig. 4 shows the magnetic hysteresis curves of undoped and Cu doped ITO nanoparticles at room temperature. The In_2O_3 and SnO_2 exhibited diamagnetic nature at room temperature. But ITO $(\text{In}_{0.95}\text{Sn}_{0.05})_2\text{O}_3$ nanoparticle exhibited ferromagnetism at room temperature and at 100 K. The clear hysteresis loop of the $(\text{In}_{0.95}\text{Sn}_{0.05})_2\text{O}_3$ nanoparticle indicates that the Curie temperature for these nanoparticles is higher than room temperature. The hysteresis loop shows a high coercive field (H_c) of 683 G. The observed magnetic moment is almost equal to that of magnetic moment observed by Peleckis et al [8] in Ni doped In_2O_3 nanoparticles prepared by solid state synthesis route method.

Transition metal doped SnO₂ and In₂O₃ exhibited room temperature ferromagnetism in our earlier studies. In the present study, tin doped In₂O₃ (ITO) nanoparticles also exhibited room temperature ferromagnetism. The (In_{0.90}Sn_{0.05}Cu_{0.05})₂O₃ nanoparticles also exhibited room temperature ferromagnetism but the strength of magnetization decreased in (In_{0.90}Sn_{0.05}Cu_{0.05})₂O₃ nanoparticles.

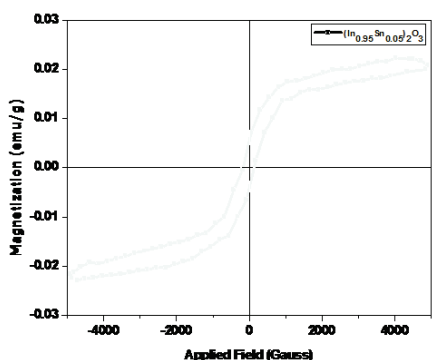


FIGURE 5. Magnetic hysteresis loops (M–H) of ITO nanoparticles at 100 K.

The samples exhibited the saturation magnetic moment (M_s) of 0.05 emu/g, coercivity (H_c) of 683 G and retentivity (M_r) of 0.02 emu/g, respectively. Whereas the strength of magnetization decreased in Cu doped ITO nanoparticles. The observed saturation magnetic moments are better than that of saturation magnetic moment of Co doped SnO₂ nanoparticles prepared by co-precipitation method [9]. Fig .5 shows the M-H curve of ITO nanoparticles at 100 K. From the figure it is clear that the saturation magnetic moment decreased at lower temperature. it may be due to antiferromagnetic or ferrimagnetism developed at low temperature. Room temperature ferromagnetism was also found in nanoparticles of nonmagnetic oxides such as CeO₂, Al₂O₃, ZnO, In₂O₃ and SnO₂ [10]; however, the corresponding bulk samples obtained by sintering the nanoparticles at high temperatures in air or oxygen became diamagnetic. The origin of ferromagnetism in these nanoscale materials is assumed to be the exchange interactions between localized electron spin moments resulting from the oxygen vacancies [11]. Recent results indicated that surface ferromagnetic states and spin polarization were realized in the presence of vacancies on the surface of In₂O₃ and Indium-Tin oxide (ITO) [12]. The less magnetic moment in polycrystalline ITO may be due to sintering of the samples in air at different higher temperatures. In the present study the samples were sintered in vacuum in which oxygen vacancies can be produced easily.

However, until now, no experiments have been performed to demonstrate the existence of surface ferromagnetism and spin polarization on the surface of undoped oxide. Room temperature ferromagnetism was also observed in Fe doped ITO thin films and concluded that the observed ferromagnetism is due to oxygen vacancies [13].

CONCLUSION

ITO (In_{0.95}Sn_{0.05})₂O₃ and Cu doped ITO (In_{0.90}Sn_{0.05}Cu_{0.05})₂O₃ nanoparticles were prepared using standard solid state reaction method and studied the structural, optical and magnetic properties systematically. The ITO and Cu doped ITO nanoparticles exhibited ferromagnetism at room temperature and the strength of the magnetic moment decreased after doping Cu into ITO lattice.

ACKNOWLEDGMENTS

Authors are thankful to VIT-SIF for providing XRD and diffused reflectance spectra (DRS) facilities.

REFERENCES

1. T. Dietl, H. Ohno and F. Matsukura, *Science* **287**, 1019-22 (2000).
2. K. Ueda, H. Tabata and T. Kawai, *Appl. Phys. Lett* **79**, 988-990 (2001).
3. Q. Wang, Q. Sun and P. Jena *Phys. Rev B* **70**, 052408-1 (2004).
4. H. Akai, *Phys Rev Lett* **81**, 3002-3005 (1998).
5. J.M.D. Coey, M. Venkatesan and C.B. Fitzgerald *Nat. Mater* **4**, 173-179 (2004).
6. S. Lacombe, H. Cardy, N. Soggiu, S. Blanc, J.L.H. Jivan and J. Ph Soumillon, *Microporous Mesoporous Mater* **46**, 311–325 (2001)
7. J. Tauc, Amorphous and Liquid Semiconductors. Plenum Press. New York (1974)
8. G. Peleckis, X. Wang and S.X. Dou, *Appl. Phys. Lett* **89**, 022501-3 (2006).
9. S. Zhuang, X. Xu, Y. Pang, H.Li, B. Yu and J.Hu, *J. Magn. Magn. Mater* **327**, 24-27 (2013).
10. C.D. Pemmaraju and S. Sanvito, *Phys. Rev. Lett.* **94**, 217205-217208 (2005).
11. H.S. Majumdar, S. Majumdar, D. Tobjork and R. Osterbacka, *Synthetic Mater* **160**, 303-306 (2010).
12. B. Xia, Y. Wu, H.W. Ho, C. Ke, W.D. Song, C.H.A. Huan, J.L. Kuo, W.G. Zhu and L. Wang, *Physica B* **406**, 3166–3169 (2011).
13. X. Pengfei, C. Yanxu and S. Shaohua, *J. Semi. Cond.* **34**, 023002-4 (2013).